ResearchGate

See discussions, stats, and author profiles for this publication at: https://www.researchgate.net/publication/235776012

Probing multifractality in tissue refractive index: Prospects for precancer detection

Article *in* Optics Letters · January 2013

DOI: 10.1364/OL.38.000211 · Source: PubMed

CITATIONS
46

READS
398

9 authors, including:

Nandan Das
Linköping University
37 PUBLICATIONS **391** CITATIONS
SEE PROFILE

Subhasri Chatterjee
TCS Research and Inovation
27 PUBLICATIONS **236** CITATIONS
SEE PROFILE

Jalpa Soni
University of Gothenburg
31 PUBLICATIONS **445** CITATIONS
SEE PROFILE

Jaidip Jagtap
Mayo Clinic - Rochester
50 PUBLICATIONS **367** CITATIONS
SEE PROFILE

Some of the authors of this publication are also working on these related projects:

Polynomial algebras View project

Machine Learning in Precancer Detection View project

All content following this page was uploaded by Jaidip Jagtap on 02 June 2014.

The user has requested enhancement of the downloaded file.

Probing multifractality in tissue refractive index: prospects for precancer detection

Nandan Das,[1] Subhasri Chatterjee,[1] Jalpa Soni,[1] Jaidip Jagtap,[2] Asima Pradhan,[2] Tapas K. Sengupta,[1] Prasanta K. Panigrahi,[1] I. Alex Vitkin,[3] and Nirmalya Ghosh[1,*]

[1]*IISER—Kolkata, BCKV Main Campus, Mohanpur, Nadia, West Bengal 741252, India*

[2]*Department of Physics, IIT Kanpur, Kanpur 208016, India*

[3]*Ontario Cancer Institute, Department of Medical Biophysics, University of Toronto, Ontario M5G 2M9, Canada*

**Corresponding author: nghosh@iiserkol.ac.in*

Received October 8, 2012; revised December 11, 2012; accepted December 11, 2012; posted December 13, 2012 (Doc. ID 177674); published January 14, 2013

Multiresolution analysis on the spatial refractive index inhomogeneities in the epithelium and connective tissue regions of a human cervix reveals a clear signature of multifractality. Importantly, the derived multifractal parameters, namely, the generalized Hurst exponent and the width of the singularity spectrum, derived via multifractal detrended fluctuation analysis, shows interesting differences between tissues having different grades of precancers. The refractive-index fluctuations are found to be more anticorrelated, and the strength of multifractality is observed to be considerably stronger in the higher grades of precancers. These observations on the multifractal nature of tissue refractive-index variations may prove to be valuable for developing light-scattering approaches for noninvasive diagnosis of precancer and early-stage cancer. © 2013 Optical Society of America

OCIS codes: 170.0170, 170.6935, 170.4580, 170.6510, 170.3880, 290.0290.

Light scattering in biological tissue originates from spatial fluctuations of local refractive index (RI) in both the cellular and the extracellular compartments, with the spatial scale of fluctuations ranging from several nanometers to several micrometers [1–4]. For many types of tissues, the spatial-scaling distribution of RI exhibits statistical self-similarity (fractality), and accordingly the scale-invariant inverse-power-law dependence of the elastic scattering signal (on either the wavelength or the angular variation of scattering) has been attributed to this self-similarity [2–5]. Recent studies have explored light-scattering models for quantification of the fractal micro-optical properties, namely, Hurst exponent (H) and fractal dimension (D_f), for their potential applications in precancer detection [5–8]. Such models are usually based on a *monofractal* hypothesis, which assumes that the scaling properties of the RI spatial fluctuations are the same over the entire tissue region probed. However, considering the wide range of dimensions of inhomogeneities and the complex nature of the spatial correlations, the monofractal approximation may be unrealistic for many tissues. It is thus desirable to study and quantify the nature of multifractality of tissue RI (spatial) variations using a more general type of statistical multiresolution analysis. A multifractal signal is typically characterized by long-range correlations, nonstationarity in fluctuations, and different local scaling behavior [9]. This type of multiresolution analysis may yield additional diagnostic information, and the multifractal parameters may potentially serve as useful metrics for precancer detection. Moreover, information obtained from such studies may help in developing appropriate models for extraction and quantification of tissue multifractality from light-scattering signals.

We have therefore analyzed the spatial RI variations of human cervical tissues (in epithelium and connective-tissue layers) having different grades of precancers by a state-of-the-art tool for multifractal research, the multifractal detrended fluctuation analysis (MFDFA) [9]. In addition to exploring the well-accepted malignant progression of the epithelial cellular compartment of most tumors, our investigations on the connective tissue (stroma) morphology are motivated by the recent findings that the progression of cancer involves altered interactions between epithelial cells and the underlying stroma, and changes in stromal biology may precede and stimulate neoplastic progression in preinvasive disease [10]. Quantification of the complex fractal-like architecture of stromal fibrous network may thus prove to be beneficial for this purpose.

We used a differential interference contrast (DIC) microscope (Olympus IX81, USA) to measure the spatial distribution of tissue RI. The tissues were histopathologically characterized (CIN or dysplasia grade I, II, and III) biopsy samples of human cervical tissues obtained from G. S. V. M. Medical College and Hospital in Kanpur, India. The unstained tissue sections (thickness ~5 μm, lateral dimension ~4 mm × 6 mm) were prepared on glass slides. The standard method employed was tissue dehydration, embedding in wax, sectioning under a rotary microtome, and subsequent dewaxing. Images were obtained separately from the epithelium and the connective tissue regions at a magnification of 60× and recorded using a CCD camera (ORCA-ERG, Hamamatsu) having 1344 × 1024 pixels (pixel dimension 6.45 μm). The width of the point spread function of the microscope was ~0.36 μm. The recorded images were unfolded (pixel-wise) in one linear direction to obtain one-dimensional fluctuation series representing the spatial variation of tissue RI. These were then analyzed through (1) Fourier analysis and (2) MFDFA.

For one-dimensional fluctuation series exhibiting statistical self-similarity, the Fourier power spectrum assumes a form of the power law ($P(\nu) \approx \nu^{-\beta}$, ν being the spatial frequency, here in μm^{-1}) at the limit of large frequencies ν [2]. Here, the power-law coefficient is

 © 2013 Optical Society of America

related to the Hurst exponent as $\beta = 2H + 1$ [9]. In Fig. 1, we show the results of the Fourier analysis on the spatial variation of RI from the connective-tissue regions of typical dysplastic cervix. The DIC images of grade I and III tissues are shown in Figs. 1(a) and 1(c), respectively. The corresponding Fourier power spectra of the generated one-dimensional spatial index fluctuations are shown in Figs. 1(b) and 1(d).

Several interesting trends can be discerned from the power spectra, which exhibit power-law scaling beyond a certain spatial frequency ν range (for $\nu \geq 0.075\ \mu m^{-1}$, the spectral density appears linear on a log–log plot). The power spectra are also associated with large background fluctuations indicating the overall randomness of the underlying index variations. Interestingly, the power-law coefficient is not uniform throughout the entire ν range. For example, the data fitted to two different selected ν ranges [lower (red) and higher (green)] yielded different values for the power-law exponent. This behavior is a manifestation of the hidden multifractality. Nevertheless, overall fitting on the broad range of ν resulted in differences in the values for the average Hurst exponents, $H = 0.255$ and 0.20 for grades I and III connective tissues, respectively. Note that the limiting values of H, unity and zero, correspond to a smooth Euclidean random field (marginal fractal) and a space-filling field (extreme fractal), respectively [7]. A lower value of H thus indicates increasing roughness of the medium (extreme fractality). However, the complex nature of the nonlinearity in the Fourier space of the spatial fluctuations of RI necessitates the use of multifractal analysis. These were therefore subjected to the MFDFA analysis, as detailed elsewhere [9].

Briefly, the profile $Y(i)$ (spatial series of length N, $i = 1 \ldots N$) is first generated from the one-dimensional spatial index fluctuations. The profile is then divided into $N_s = \mathrm{int}(N/s)$ nonoverlapping segments b of equal length s. The local trend of the series ($y_b(i)$) is determined for each segment b by least-square polynomial

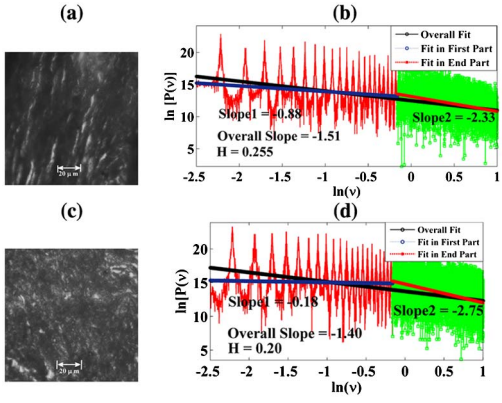

Fig. 1. (Color online) DIC images of typical (a) grade I and (c) grade III dysplastic connective tissues. The corresponding Fourier power spectra are shown in (b) and (d), respectively (in natural logarithm scale). The two different selected ν ranges (lower and higher) exhibiting different power-law scaling are shown by red and green colors. The fits at the lower ν range (blue line), at the higher ν range (red line), and the overall fit (black line). The values for the power-law coefficients (slope $-\beta$) and the corresponding estimate for the average Hurst exponents H (for overall fitting) are noted.

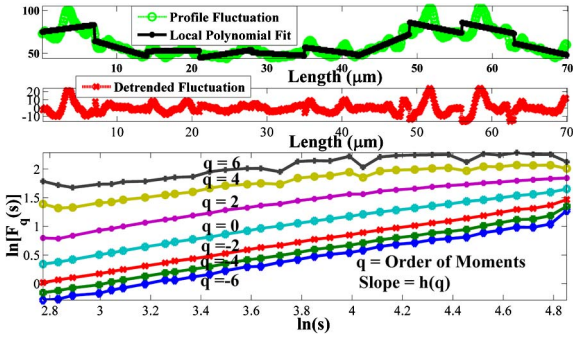

Fig. 2. (Color online) MFDFA analysis for grade I dysplastic connective tissue. The profile $Y(i)$ (green dashed curve) and the local polynomial fit $y_b(i)$ of Eq. (1) (black solid curve), polynomial of degree 1, is shown here for a particular segment corresponding to a typical window size $s = 65$ (top panel). The detrended fluctuations (for $s = 65$) is displayed in the middle panel. The x axis represents the actual length scale (in micrometers). The log–log (natural logarithm) plot of the moment ($q = -6$ to $+6$) dependent fluctuation function $F_q(s)$ versus s [derived using Eq. (2)] is shown in the bottom panel.

fitting and then subtracted from the segmented profiles to yield the detrended fluctuations. The resulting variance is determined for each segment as

$$F^2(b,s) = \frac{1}{s}\sum_{i=1}^{s}[Y\{(b-1)s+i\} - y_b(i)]^2. \quad (1)$$

The moment (q) dependent fluctuation function is then extracted by averaging over all the segments as

$$F_q(s) = \left\{\frac{1}{2N_s}\sum_{b=1}^{2N_s}[F^2(b,s)]^{q/2}N\right\}^{1/q}. \quad (2)$$

The procedure was performed twice on the series, starting from either end of the series [9]. The scaling behavior is subsequently determined by analyzing the variations of $F_q(s)$ versus s for each value of q, assuming the general scaling function as

$$F_q(s) \sim s^{h(q)}. \quad (3)$$

Here, the generalized Hurst exponent $h(q)$ and the classical multifractal scaling exponent $\tau(q)$ are related by

$$\tau(q) = qh(q) - 1. \quad (4)$$

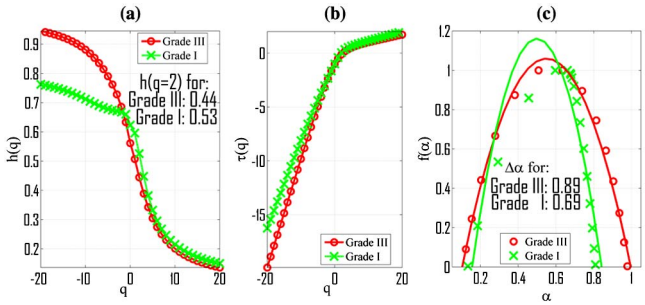

Fig. 3. (Color online) Comparison of the variation of (a) generalized Hurst exponent $h(q)$, derived (using Eq. 3), (b) classical multifractal scaling exponent $\tau(q)$ (derived via Eq. 4), and (c) the singularity spectrum $f(\alpha)$(derived using Eq. 5) for grade I and grade III dysplastic connective tissues.

Table 1. Summary of MFDFA Analysis on RI Fluctuations of Cervical Tissues

Tissue Region	Generalized Hurst Exponent [$h(q=2)$]			Width of Singularity Spectrum ($\Delta\alpha$)		
	Grade I	Grade II	Grade III	Grade I	Grade II	Grade III
Connective tissue	0.54 ± 0.03	0.50 ± 0.04	0.36 ± 0.08	0.60 ± 0.10	0.68 ± 0.13	0.88 ± 0.07
Epithelium	0.55 ± 0.09	0.54 ± 0.02	0.50 ± 0.03	0.60 ± 0.09	0.72 ± 0.16	0.73 ± 0.10

Note that for a stationary, monofractal series $h(q=2)$, is identical to the Hurst exponent H. Here, values of $H = 0.5$, >0.5, and <0.5 correspond to uncorrelated random, long-range correlated, and anticorrelated behavior, respectively. The two sets of the scaling exponents $h(q)$ and $\tau(q)$ along with the singularity spectrum $f(\alpha)$ completely characterize any nonstationary, multifractal fluctuation series. Here, $f(\alpha)$ is related to $\tau(q)$ via a Legendre transformation:

$$\alpha = \frac{d\tau}{dq}, \qquad f(\alpha) = q\alpha - \tau(q), \tag{5}$$

where α is the singularity strength and the width of $f(\alpha)$ a quantitative measure of multifractality [9].

The results of the MFDFA analysis performed on the spatial RI fluctuations of the two tissues are shown in Figs. 2 and 3. Figure 2 displays the various steps of the multiresolution analysis for the grade I dysplastic connective tissue. The presence of various large- and small-scale index fluctuations are apparent in the profile $Y(i)$ (top panel). The detrending procedure (middle panel) removes the relatively broader local trends and enhances the smaller fluctuations. The resulting slope of the log–log plot of the fluctuation function $F_q(s)$ versus s is observed to vary significantly with varying moment q (bottom panel). This is clear evidence of multifractality.

Figure 3 shows a comparison of $h(q)$, $\tau(q)$ and $f(\alpha)$ for the grade I and III connective tissues. Clearly, multifractality is manifested as significant variations of $h(q)$ versus q and the resulting width of the singularity spectrum for both tissue types. The values for $h(q=2)$ for the grade I and III tissues are 0.53 and 0.44, respectively. Lower values of $h(q=2)$ (<0.5) signify that the spatial index fluctuations are more anticorrelated at the higher grades of precancer. Even though the qualitative trends of the MFDFA-derived $h(q=2)$ values for the grade I and III tissues are similar to the Hurst exponent (H) determined using the Fourier analysis (decrease at higher grades of precancer), there exist significant differences. These are caused by the nonstationarity hidden in the spatial fluctuations of tissue RI and underscore the inadequacy of Fourier analysis for quantification of self-similarity of such complex multifractal fluctuations. Interestingly, the differences in the variations of $h(q)$ between the grade I and the grade III tissues are more prominent for negative values of the moment q [Fig. 3(a)], which implies the relative importance of the small-scale index fluctuations. This follows from the fact that negative values of the moment q influence the small fluctuations, whereas positive values influence large fluctuations [9]. The resulting width of the singularity spectrum is significantly higher for the grade III tissue ($\Delta\alpha = 0.89$) as compared to the grade I tissue ($\Delta\alpha = 0.69$) [Fig. 3(c)], indicating stronger multifractality in the higher grades of precancer. As noted previously, lower values of $h(q=2)$ in the grade III connective tissue is indicative of predominance of index inhomogeneities having smaller spatial dimensions. This, together with the observation of a larger difference in $h(q)$ for negative q values (between different grades), points toward morphological alterations associated with the microarchitecture of the fibrous network. This may originate from the fact that the volume fraction of the fibrous network in the connective tissue decreases with precancer and cancer progression, and fibers tend to be shorter in neoplastic stroma [10]. Increased heterogeneity of such fibrous networks may also manifest as stronger multifractality in the corresponding spatial RI fluctuations.

Analysis performed on epithelial (cellular) regions of the same tissues also showed a clear signature of multifractality. However, the differences between different grades were less pronounced for the epithelium. The results of the MFDFA analysis performed on 10 pathologically graded cervical tissue specimens are summarized in Table 1. Clear trends are apparent, specifically for the connective-tissue regions. The higher grades of precancers consistently show a lower value of the generalized Hurst exponent $h(q=2)$ and a larger width of the singularity spectrum $\Delta\alpha$.

To summarize, multiresolution analysis revealed distinct indications of multifractality in the spatial variations of RI in human cervical tissues, with the strength of multifractality being significantly higher in the higher grades of precancers. Moreover, the index fluctuations were more anticorrelated in the higher grades. In contrast to previous tissue light-scattering analyses in the monofractal approximation [2–8], the results reported here underscore the need for incorporation of the complex multifractal correlations in the models. Initial results also indicate that tissue multifractality may provide additional targets to aid in screening and detection of precancerous changes.

References

1. V. V. Tuchin, L. Wang, and D. À. Zimnyakov, *Optical Polarization in Biomedical Applications* (Springer-Verlag, 2006).
2. J. M. Schmitt and G. Kumar, Opt. Lett. **21**, 1310 (1996).
3. N. N. Boustany, S. A. Boppart, and V. Backman, Annu. Rev. Biomed. Eng. **12**, 285 (2010).
4. A. Wax and V. Backman, eds., *Biomedical Applications of Light Scattering* (McGraw-Hill, 2009).
5. M. Hunter, V. Backman, G. Popescu, M. Kalashnikov, C. W. Boone, A. Wax, V. Gopal, K. Badizadegan, G. D. Stoner, and M. S. Feld, Phys. Rev. Lett. **97**, 138102 (2006).
6. M. Xu and R. R. Alfano, Opt. Lett. **30**, 3051 (2005).
7. C. J. R. Sheppard, Opt. Lett. **32**, 142 (2007).
8. I. R. Capoglu, J. D. Rogers, A. Taflove, and V. Backman, Opt. Lett. **34**, 2679 (2009).
9. J. W. Kantelhardt, S. A. Zschiegner, E. Koscielny-Bunde, S. Havlin, A. Bunde, S. Havlin, and H. E. Stanley, Physica A **316**, 87 (2002).
10. N. Thekkek and R. Richards-Kortum, Nat. Rev. Cancer **8**, 725 (2008).

View publication stats